Letter

Enlarged Kuramoto model: Secondary instability and transition to collective chaos

Iván León and Diego Pazó
Instituto de Física de Cantabria (IFCA), Universidad de Cantabria-CSIC, 39005 Santander, Spain

(Received 2 September 2021; accepted 21 March 2022; published 11 April 2022)

The emergence of collective synchrony from an incoherent state is a phenomenon essentially described by the Kuramoto model. This canonical model was derived perturbatively, by applying phase reduction to an ensemble of heterogeneous, globally coupled Stuart-Landau oscillators. This derivation neglects nonlinearities in the coupling constant. We show here that a comprehensive analysis requires extending the Kuramoto model up to quadratic order. This "enlarged Kuramoto model" comprises three-body (nonpairwise) interactions, which induce strikingly complex phenomenology at certain parameter values. As the coupling is increased, a secondary instability renders the synchronized state unstable, and subsequent bifurcations lead to collective chaos. An efficient numerical study of the thermodynamic limit, valid for Gaussian heterogeneity, is carried out by means of a Fourier-Hermite decomposition of the oscillator density.

DOI: 10.1103/PhysRevE.105.L042201

Collective synchronization is a phenomenon in which an ensemble of heterogeneous, self-sustained oscillatory units (commonly known as oscillators) spontaneously entrain their rhythms. This is a pervasive phenomenon observed in natural systems and man-made devices, covering a wide range of spatiotemporal scales, from cell aggregates to swarms of fireflies [1,2].

Seeking to understand the onset of collective synchronization, Winfree invented a model consisting of globally coupled oscillatory units with one degree of freedom (phase oscillators) [3,4]. Following this scheme, Kuramoto found an analytically tractable model, which captures the onset of collective synchronization from an incoherent state [5,6]. Due to its simplicity, the Kuramoto model and its generalization with phase-lagged coupling—the so-called Kuramoto-Sakaguchi model after Ref. [7]—have been intensely studied, with a vast number of extensions and applications in several fields [8,9].

The Kuramoto(-Sakaguchi) model is often introduced as above, i.e., as a mere mathematical refinement of the Winfree model. However, this is only partly true, since Kuramoto rigorously derived the model bearing his name. In particular, he applied phase reduction to an ensemble of weakly coupled Stuart-Landau oscillators [5,6]. The Stuart-Landau oscillator is a relevant natural choice, as it represents a generic limit-cycle attractor close to a Hopf bifurcation.

Kuramoto's perturbative phase-reduction approach is valid for weak coupling. Specifically, oscillator heterogeneity and interactions appear at zeroth and linear orders in the coupling constant, respectively. These considerations explain why the quadratic order was neglected in the original Kuramoto model. Nevertheless, in certain circumstances, going beyond the first (or linear) order may be required. Indeed, the descriptions of some experiments with lattices of optomechanical [10] and nanoelectromechanical [11] oscillators rely on second-order phase reductions. The analysis of the corresponding second-order phase-reduced models has remained, however, rather incomplete. The reason for this is the nonpairwise interactions appearing at quadratic order. From this perspective, the original setup with heterogeneous, diffusively coupled Stuart-Landau oscillators appears to be the ideal testbed model for investigating second-order phase reduction to the fullest extent possible. So far, only the case of identical oscillators has been analyzed [12].

Recently, nonpairwise (also called "higher-order") interactions have attracted growing attention in several fields, such as neuroscience, ecology, and social systems (see Refs. [13,14] and references therein). In this spirit, several works have considered populations of phase oscillators with nonpairwise interactions from the outset. Simplifying *ad hoc* assumptions, such as absent pairwise coupling [15–18] and/or particularly convenient nonpairwise interactions [18–21] (e.g., admitting the Ott-Antonsen ansatz [22]), are adopted seeking analytical tractability.

In this Research Letter we extend the Kuramoto model up to second order in the coupling constant ϵ. In this "enlarged" Kuramoto model the new terms of order ϵ^2 comprise two different three-body (nonpairwise) interactions. Strikingly, their combined action triggers a secondary instability in which standard collective synchronization destabilizes. This is the precursor of a sequence of instabilities giving rise to a state of collective chaos. We efficiently investigate the thermodynamic limit of the model by means of a Fourier-Hermite decomposition of the oscillator density. This scheme appeared some years ago in a theoretical study [23], but it is numerically implemented here (adopting an appropriate closure).

The starting point of our work is a heterogeneous population of $N \gg 1$ Stuart-Landau oscillators with global diffusive coupling:

$$\dot{A}_j = (1 + i\sigma\omega_j)A_j - (1+ic_2)|A_j|^2 A_j + \epsilon(1 + ic_1)(\overline{A} - A_j). \quad (1)$$

Here, $A_j \equiv r_j e^{i\phi_j}$ is a complex variable, and index j runs from 1 to N. The ω_j's are drawn from a unit-variance normal distribution $g(\omega)$. The mean of $g(\omega)$ is selected to be 0, by going to a rotating frame if necessary. Therefore each individual Stuart-Landau oscillator possesses a natural frequency equal to $\sigma\omega_j - c_2$, where c_2 is the nonisochronicity parameter. Parameter $\sigma > 0$ is included to account for the frequency dispersion. Concerning the coupling, it is diffusive through the mean field $\overline{A} = \frac{1}{N}\sum_{i=1}^{N} A_i$. Parameter $\epsilon > 0$ controls the coupling strength, and c_1 modulates its reactivity. We are exclusively interested in the thermodynamic limit ($N \to \infty$) of the model. In this Research Letter we select $\sigma = 10^{-3}$ and $c_2 = 3$ (a standard value in the literature, see, e.g., Ref. [24]), leaving c_1 and ϵ as control parameters. The effect of varying c_2 and σ is discussed at the end of this Research Letter.

System (1) displays a plethora of complex states. In particular, collective chaos already emerges at moderate and large coupling under simplifying assumptions such as homogeneity ($\sigma = 0$) [24,25] and vanishing reactivity and shear ($c_1 = c_2 = 0$) [26]. We focus here on the weak-coupling regime, in which the oscillators remain close to their original limit cycles at $r_j = 1$ and a phase description becomes possible. Two states are generically expected for small ϵ. On the one hand, there is the uniform incoherent state (UIS), corresponding to a vanishing mean field $\overline{A}$ (in the thermodynamic limit), with the oscillator angles ϕ_j uniformly scattered; see Figs. 1(a) and 1(b) for particular parameter values and $\epsilon = 0.07$. On the other hand, typically, as ϵ exceeds a certain threshold, UIS becomes unstable, and a state of collective partial synchrony (PS) emerges. In this configuration, a macroscopic proportion of the oscillators becomes entrained to a common frequency $\langle\dot{\phi}_{j\in S}\rangle = \Omega$, and the mean field rotates uniformly with constant amplitude: $|\overline{A}| = \text{const}$. In a finite population, as in Fig. 1(c), entrained oscillators may not be observed, since they belong to one of the tails of $g(\omega)$. Drifting oscillators alone cause $\overline{A}$ to depart from zero. Surprisingly, our numerical simulations indicate that the dynamics may become of a different kind as the coupling is further increased, while still remaining small. As shown in Fig. 1(a) for $\epsilon = 0.09$, the collective dynamics incorporates a new frequency, and $|\overline{A}(t)|$ oscillates periodically, i.e., the attractor is a two-dimensional torus or T^2 (disregarding finite-size fluctuations). Figure 1(d) shows the corresponding snapshot of the angles ϕ_j for $\epsilon = 0.09$. We may see that part of the population forms a two-cluster state that evolves in time such that the phase differences are time dependent but bounded. It is very much like the Bellerophon state coined in Ref. [27] for ensembles of phase oscillators. For still larger ϵ, $|\overline{A}|$ exhibits even more complex oscillations, as can be seen setting $\epsilon = 0.115$ in Fig. 1(a). In Fig. 1(f) we represent the local maxima and minima of $|\overline{A}(t)|$ as a function of ϵ. The low-frequency modulation sets in at $\epsilon \approx 0.109$. As a result of the instability, a three-frequency quasiperiodic collective motion is, in principle, expected. Still, an additional transition to weak collective chaos cannot be ruled out. At some parameter values (e.g., $\epsilon = 0.14$, $c_1 = -0.415$; see Supplemental Material [28]), the largest Lyapunov exponent does not decay to zero with the system size, which is a clear indication of collective chaos. (For the value $\epsilon = 0.115$ taken in Fig. 1 the result is inconclusive.)

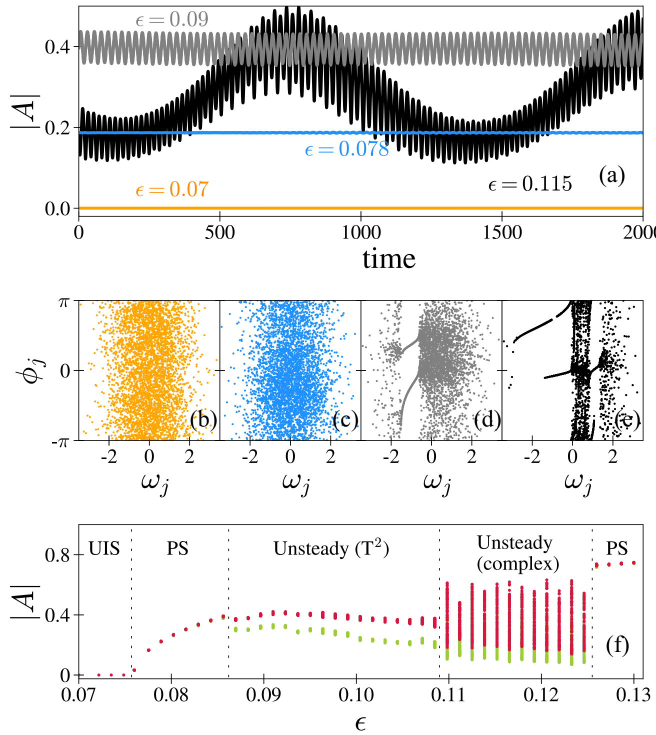

FIG. 1. Dynamics of the population of 20 000 Stuart-Landau oscillators [Eq. (1)] for different values of ϵ with $c_1 = -0.4$, $c_2 = 3$, and $\sigma = 10^{-3}$. (a) Time series of the mean-field amplitude $|\overline{A}|$ for $\epsilon = 0.07$, 0.078, 0.09, and 0.115. $|\overline{A}| \simeq 0$, $|\overline{A}| \simeq \text{const} > 0$, and periodic $|\overline{A}(t)|$ correspond to the UIS, PS, and quasiperiodic global attractor, respectively. (b)–(e) Snapshots of the angular variables ϕ_j for each of the four ϵ values chosen in (a). Only a subset of 4000 oscillators are shown for clarity. (f) Local maxima and minima of $|\overline{A}|$ as constant ϵ is increased by steps of size 1.35×10^{-3}.

To put the previous observations in a wider framework, we numerically determined where the unsteady behavior occurs in the c_1-ϵ plane. The phase diagram in Fig. 2(a) shows where qualitatively different dynamics are observed. The stability boundary of the UIS was analytically computed following the approach in Ref. [29]; see Supplemental Material. Remarkably, numerical simulations of Eq. (1) reveal that PS is unstable inside the dark shaded region in Fig. 2(a), i.e., unsteady $|\overline{A}(t)|$ spontaneously sets in. In addition, numerical continuation discloses an adjacent narrow band of coexistence between unsteady dynamics and PS. The orange line in Fig. 2(a) divides the unsteady region into two parts: the lower one with T^2 collective motion, and the upper one with more complex oscillations. We emphasize that determining the exact nature of the complex unsteady states is an arduous work, which hinders a more detailed phase diagram.

At this point, we resort to phase reduction in order to better understand the nature and organization of the unsteady collective states. For weak coupling, phase reduction allows us to describe the system solely in terms of phase variables $\theta_j = \phi_j - c_2 \ln r_j$ [2,6]. Following Ref. [12], we write down the second-order phase reduction [30] of (1), or the "enlarged Kuramoto model":

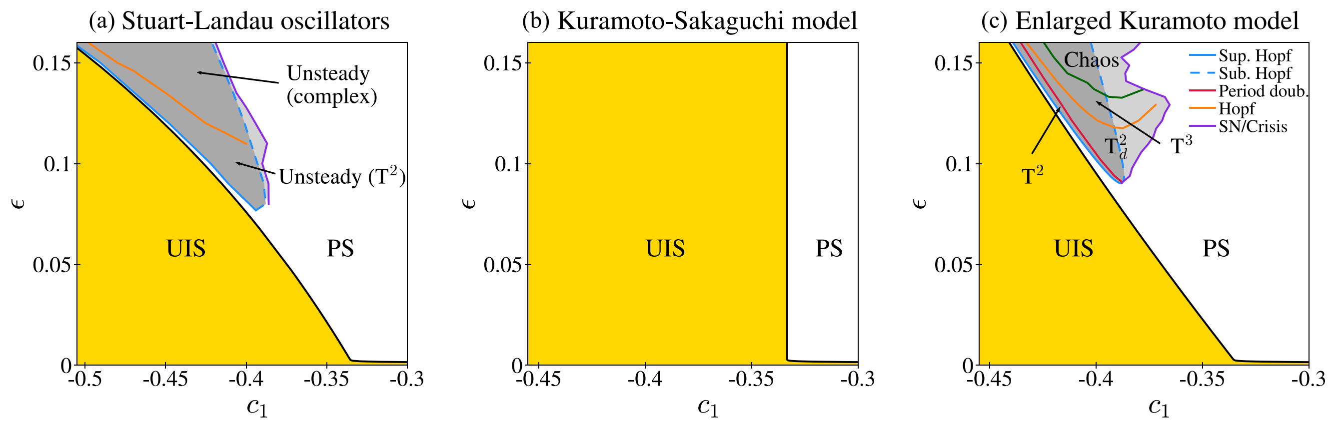

FIG. 2. Phase diagrams of model (1) for $c_2 = 3$ and $\sigma = 10^{-3}$, as well as its first- and second-order phase reductions. (a) Model (1): All boundaries were obtained from numerical simulations with a population of $N = 20\,000$ Stuart-Landau oscillators, save the boundary of the UIS (obtained analytically). In the dark shaded region, the UIS and PS are both unstable, and $|\bar{A}|$ varies with time. In the light shaded region, PS coexists with an unsteady state. (b) Kuramoto-Sakaguchi model obtained from Eq. (2) discarding quadratic terms in ϵ. (c) Enlarged Kuramoto model [Eq. (2)]; all boundaries, except the UIS-PS line, were determined using Eq. (5). The right boundary of the bistability region (in purple) indicates where the attractor with unsteady dynamics abruptly disappears, indistinctively through a saddle-node bifurcation of tori, a boundary crisis, or any other bifurcation. Sup., supercritical; Sub., subcritical; doubl., doubling; SN, saddle-node bifurcation.

$$\dot{\theta}_j = \sigma\omega_j + \epsilon\eta R \sin(\Psi - \theta_j + \alpha) + \frac{\epsilon^2\eta^2}{4}[R\sin(\Psi - \theta_j + \beta) - R^2\sin(2\Psi - 2\theta_j + \beta) + R\,Q\sin(\Phi - \Psi - \theta_j)], \tag{2}$$

where three new constants, depending on c_1 and c_2, are defined: $\eta \equiv \sqrt{(1+c_2^2)(1+c_1^2)}$ and the phase lags $\alpha \equiv \arg[1 + c_1c_2 + (c_1 - c_2)i]$ and $\beta \equiv \arg(1 - c_1^2 + 2c_1 i)$. For simplicity, we have chosen a reference frame with vanishing central frequency. Interactions involve two mean fields, $Z_1 \equiv R\,e^{i\Psi}$ and $Z_2 \equiv Q\,e^{i\Phi}$, which are the first two elements of an infinite set of Kuramoto-Daido order parameters [31]: $Z_k \equiv N^{-1}\sum_{j=1}^{N} e^{ik\theta_j}$. Equation (2) includes nonpairwise interactions, which are inherent to higher-order phase reduction, even if the coupling in the original system (1) is pairwise and linear [12,32,33]. In particular, three-body interactions are conveyed by the last two terms [34] and are comparatively weak (of order ϵ^2), as usual in physics [35]. This is not the case in most previous studies of coupled phase oscillators [15–17,19,20,36,37], but see Refs. [11,12,33,38].

We start the analysis of Eq. (2) noticing that if we neglect the $O(\epsilon^2)$ terms, then we recover the Kuramoto-Sakaguchi model with coupling constant $\epsilon\eta$. For $N \to \infty$, the phase diagram resulting from this $O(\epsilon)$ approximation is shown in Fig. 2(b). The only attracting configurations are the UIS and PS. The boundary of the UIS can be calculated following Ref. [7]. It diverges at $c_1 = -c_2^{-1} = -1/3$, corresponding to $\alpha = -\pi/2$. When comparing Figs. 2(a) and 2(b), it is manifest that first-order phase reduction does not provide a faithful description of system (1) in the left part of the phase diagram.

We now consider Eq. (2) in full. Concerning the linear stability of the UIS ($R = Q = 0$), only the first term of order ϵ^2 is relevant. It may be added to the linear term to recalculate the stability boundary [7]; see Supplemental Material. The result is shown as a solid black line in Fig. 2(c). Now the boundary of the UIS exhibits a knee at $c_1 \approx -1/3$, in qualitative agreement with Fig. 2(a). Analyzing the stability of PS is a much harder problem. Through a numerical self-consistent approach [7] we tracked the branch of PS emanating from incoherence. However, this does not allow us to determine its stability. Moreover, the direct numerical integration of Eq. (2) is not more efficient than simulating Eq. (1): The number of degrees of freedom is reduced by a factor of 2, but at the cost of including computationally expensive trigonometric functions.

In order to exploit the dimensionality reduction achieved in Eq. (2), an alternative strategy is required. We resort to a moments system introduced almost a decade ago by Chiba in his theoretical study of the Kuramoto model [23]. Crucially, working with a set of moments avoids finite-size fluctuations and the concomitant microscopic (phase) chaos [39]. We start by defining the density $\rho(\theta|\omega,t)$ such that $\rho(\theta|\omega,t)d\theta$ is the fraction of oscillators with phases between θ and $\theta + d\theta$ and frequency ω at time t. Now, we write the Fourier-Hermite decomposition of ρ:

$$\rho(\theta|\omega,t) = \frac{1}{2\pi}\sum_{k=-\infty}^{\infty}\sum_{m=0}^{\infty} P_k^m(t)e^{-ik\theta}h_m(\omega), \tag{3}$$

where $h_m(x) = \mathrm{He}_m(x)/\sqrt{m!}$ are normalized (probabilist's) Hermite polynomials: $\int_{-\infty}^{\infty} h_m(\omega)h_n(\omega)g(\omega)d\omega = \delta_{mn}$. The Fourier-Hermite coefficients P_k^m are obtained inverting Eq. (3):

$$P_k^m(t) = \int_0^{2\pi} d\theta e^{ik\theta}\int_{-\infty}^{\infty} d\omega h_m(\omega)g(\omega)\rho(\theta|\omega,t). \tag{4}$$

These Fourier-Hermite modes extend the Kuramoto-Daido order parameters to the space of the natural frequencies. Specifically, $P_k^0 = Z_k$ (in the $N \to \infty$ limit). The density ρ obeys the continuity equation $\partial_t \rho = -\partial_\theta(\rho\dot{\theta})$. Inserting the expansion (3), using the recurrence relation $\omega h_m = \sqrt{m}h_{m-1} + \sqrt{m+1}h_{m+1}$ [40], and redefining $P_k^m \to (-i)^m P_k^m$ for convenience, we get an infinite set of ordinary differential equations:

$$\begin{aligned} k^{-1}\dot{P}_k^m &= \sigma\left(\sqrt{m}P_k^{m-1} - \sqrt{m+1}P_k^{m+1}\right) \\ &+\frac{\epsilon\eta}{2}\left(P_{k-1}^m Z_1 e^{i\alpha} - P_{k+1}^m Z_1^* e^{-i\alpha}\right) \\ &+\frac{\epsilon^2\eta^2}{8}\left(P_{k-1}^m Z_1 e^{i\beta} - P_{k+1}^m Z_1^* e^{-i\beta} - P_{k-2}^m Z_1^2 e^{i\beta}\right. \\ &\left.+P_{k+2}^m Z_1^{*2} e^{-i\beta} + P_{k-1}^m Z_2 Z_1^* - P_{k+1}^m Z_2^* Z_1\right), \qquad (5) \end{aligned}$$

where the asterisk denotes complex conjugation. System (5) is equivalent to Eq. (2) with $N \to \infty$.

The numerical integration of Eq. (5) requires us to implement a truncation at finite $k_{\max}$ and $m_{\max}$, with an adequate closure. Note first that, in the UIS, $P_0^0 = 1$ is the only nonzero coefficient, whereas in the PS state the modes decay with k and m roughly as $|P_k^m| \sim e^{-ak}e^{-b\sqrt{m}}$. We imposed the boundary conditions $P_{k_{\max}+1}^m = 0$ and $P_k^{m_{\max}+1} = 2P_k^{m_{\max}} - P_k^{m_{\max}-1}$. We tested the performance of different system sizes, finding that $k_{\max} = m_{\max} = 40$ already yields an excellent convergence, even for strongly unsteady states. Therefore our analysis below relies on Eq. (5) with $n_f = k_{\max} \times (m_{\max} + 1) \times 2 = 3280$ degrees of freedom. In comparison, simulating Eq. (2) with n_f oscillators is unproductive because of unavoidable finite-size fluctuations.

One now can see that the PS state corresponds to a solid rotation $P_k^m(t) = p_k^m e^{ik\Omega t}$. After inserting this solution into Eq. (5), the unknowns p_k^m and Ω are found via a Newton-Raphson algorithm (imposing $p_1^1 \in \mathbb{R}$). The result completely agrees with the one obtained from the self-consistent numerical calculation mentioned above. Now, however, we can determine linear stability. Moving to a rotating frame with angular velocity Ω, we linearize the system around the fixed point. The locus of a secondary (Hopf) instability is accurately located requiring the eigenvalues of the Jacobian matrix with the largest real part to be $\pm i\Omega_H$ (with an extra zero eigenvalue due to rotational invariance $P_k^m \to e^{ik\gamma}P_k^m$). The Hopf line is shown in blue in Fig. 2(c). The transition is supercritical (subcritical) at the solid (dashed) line. The emerging oscillatory mode yields a torus attractor (T^2), in which, due to the rotational symmetry, no lockings on its surface are expected; see, e.g., Refs. [41,42]. Recalling Eq. (2), we infer that, at the level of the individual oscillators, the superimposed oscillation induces entrainment at frequencies $\Omega + (n/2)\Omega_H$ ($n \in \mathbb{Z}$). The half-integer frequency plateaus stem from the term accompanying R^2 in Eq. (2). In particular, the two clusters in Fig. 1(d) correspond to a frequency plateau at frequency $\Omega + \Omega_H/2$.

The remaining regions of the phase diagram in Fig. 2(c) are determined from direct numerical simulations of Eq. (5) with the aforementioned closure, as well as by computing the largest Lyapunov exponents $\{\lambda_i\}_{i=1,2,\ldots}$. Our systematic exploration reveals a period-doubling bifurcation line ($\mathrm{T}^2 \to \mathrm{T}_d^2$ transition) close to the supercritical-Hopf line. The period-doubling bifurcation line almost certainly exists also for the ensemble of Stuart-Landau oscillators. Magnifying the gray line in Fig. 1(a), the signature of a doubled torus T_d^2 can be discerned. However, it is very hard to determine the bifurcation point due to the long transients involved and unavoidable finite-size fluctuations; see Fig. 1(f).

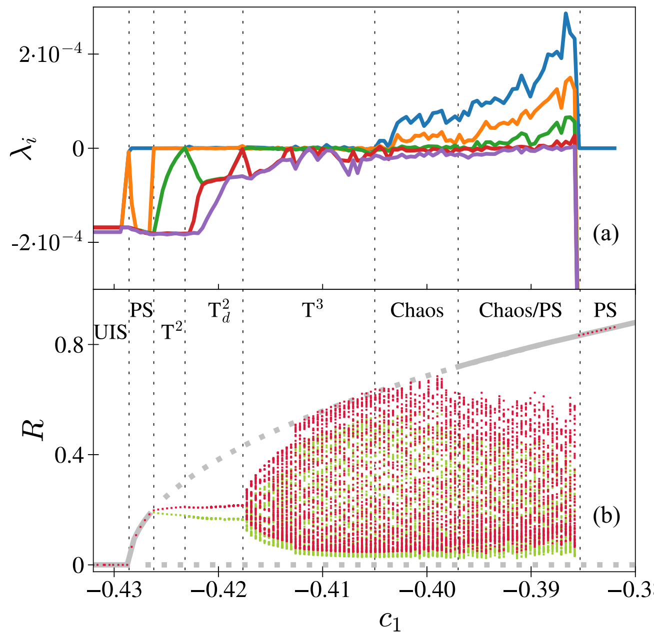

FIG. 3. Sequence of bifurcations of Eq. (2), obtained from Eq. (5), as c_1 is increased with $\epsilon = 0.14$. (a) Five largest Lyapunov exponents $\{\lambda_i\}_{i=1,\ldots,5}$. (b) Local maxima and minima of $R(t)$. As a reference, the R values of the UIS ($R = 0$) and PS ($R > 0$) are depicted in gray. Solid (dashed) lines correspond to linearly stable (unstable) states.

As occurs with the ensemble of Stuart-Landau oscillators, the torus attractor undergoes a Hopf bifurcation; see the orange line in Fig. 2(c). Thereby three-frequency quasiperiodic dynamics (T^3 attractor) emerges, consistent with three vanishing Lyapunov exponents.

Adjacent to the T^3 domain in Fig. 2(c), there exists a region with chaotic dynamics, in conformity with the Ruelle-Takens-Newhouse scenario. As occurred with system (1) [Fig. 2(a)], PS and unsteady states coexist. In Fig. 2(c) the bistability region is bounded by a purple line denoting either a saddle-node bifurcation, emanating from a (codimension-2) Bautin point at the bottom of the Hopf line, or an attractor crisis. The phase diagram in Fig. 2(c) reveals which are the unsteady collective states of (1), and their expected arrangement. Indeed, obtaining a phase diagram with the degree of detail of Fig. 2(c) is virtually unattainable simulating the original system, Eq. (1).

To better characterize the chaotic region, a detailed exploration along the horizontal line $\epsilon = 0.14$ is shown in Fig. 3. In Figs. 3(a) and 3(b) the five largest Lyapunov exponents and the local maxima and minima of $|P_1^0(t)| = R(t)$ are, respectively, depicted for the same c_1 range. In the T^3 interval there may be some additional bifurcations (lockings or torus doubling), which we did not attempt to resolve. Interestingly, in the chaotic domain an increasing number of Lyapunov exponents become positive as c_1 increases, i.e., collective chaos transforms into collective hyperchaos.

In this Research Letter we have introduced the enlarged Kuramoto model: a population of phase oscillators in which three-body interactions enter in a perturbative way. Remarkably, this makes a world of difference, drastically reshaping the traditional Kuramoto scenario. The enlarged Kuramoto model exhibits a variety of unsteady states, including collective chaos and hyperchaos. Remarkably, we report these states in a population of globally coupled phase oscillators, with a unimodal distribution of the natural frequencies. We have considered a particular frequency dispersion $\sigma = 10^{-3}$ in Fig. 2(c). If σ is lowered, the bottom of the Hopf bifurcation line approaches the c_1 axis at $c_1 = -c_2^{-1}$. This is expected to occur for any nonzero c_2 value, consistent with the $\sigma = 0$ case [12] (to be shown elsewhere). Nonetheless, only heterogeneity, in contradistinction to weak noise [12,43], is able to trigger unsteady collective dynamics (absent for $\sigma = 0$). As a final remark, we stress that reducing the population of Stuart-Landau oscillators (1) to the phase model (2) is both illuminating and convenient, as it enables an efficient investigation of the thermodynamic limit by virtue of the Fourier-Hermite expansion. The application of this scheme to other populations of phase oscillators with Gaussian heterogeneity is straightforward. For other forms of $g(\omega)$ a suitable set of orthogonal polynomials must be adopted: For example, the Fourier-Legendre mode decomposition is appropriate for uniform $g(\omega)$.

We thank Ernest Montrbrió and Juan M. López for their critical reading of the manuscript. We acknowledge support by Agencia Estatal de Investigación and Fondo Europeo de Desarrollo Regional under Project No. FIS2016-74957-P (AEI/FEDER, EU). I.L. acknowledges support by Universidad de Cantabria and Government of Cantabria under the Concepción Arenal program.

[1] S. H. Strogatz, *Sync: The Emerging Science of Spontaneous Order* (Hyperion, New York, 2003).

[2] A. S. Pikovsky, M. G. Rosenblum, and J. Kurths, *Synchronization, a Universal Concept in Nonlinear Sciences* (Cambridge University Press, Cambridge, 2001).

[3] A. T. Winfree, Biological rhythms and the behavior of populations of coupled oscillators, J. Theor. Biol. **16**, 15 (1967).

[4] A. T. Winfree, *The Geometry of Biological Time* (Springer, New York, 1980).

[5] Y. Kuramoto, Self-entrainment of a population of coupled nonlinear oscillators, in *International Symposium on Mathematical Problems in Theoretical Physics*, Lecture Notes in Physics Vol. 39, edited by H. Araki (Springer-Verlag, Berlin, 1975), pp. 420–422.

[6] Y. Kuramoto, *Chemical Oscillations, Waves, and Turbulence* (Springer-Verlag, Berlin, 1984).

[7] H. Sakaguchi and Y. Kuramoto, A soluble active rotator model showing phase transitions via mutual entrainment, Prog. Theor. Phys. **76**, 576 (1986).

[8] J. A. Acebrón, L. L. Bonilla, C. J. Pérez-Vicente, F. Ritort, and R. Spigler, The Kuramoto model: A simple paradigm for synchronization phenomena, Rev. Mod. Phys. **77**, 137 (2005).

[9] F. A. Rodrigues, T. K. DM. Peron, P. Ji, and J. Kurths, The Kuramoto model in complex networks, Phys. Rep. **610**, 1 (2016).

[10] G. Heinrich, M. Ludwig, J. Qian, B. Kubala, and F. Marquardt, Collective Dynamics in Optomechanical Arrays, Phys. Rev. Lett. **107**, 043603 (2011).

[11] M. H. Matheny, J. Emenheiser, W. Fon, A. Chapman, A. Salova, M. Rohden, J. Li, M. Hudoba de Badyn, M. Pósfai, L. Duenas-Osorio, M. Mesbahi, J. P. Crutchfield, M. C. Cross, R. M. D'Souza, and M. L. Roukes, Exotic states in a simple network of nanoelectromechanical oscillators, Science **363**, eaav7932 (2019).

[12] I. León and D. Pazó, Phase reduction beyond the first order: The case of the mean-field complex Ginzburg-Landau equation, Phys. Rev. E **100**, 012211 (2019).

[13] T. Stankovski, T. Pereira, P. V. E. McClintock, and A. Stefanovska, Coupling functions: Universal insights into dynamical interaction mechanisms, Rev. Mod. Phys. **89**, 045001 (2017).

[14] F. Battiston, G. Cencetti, I. Iacopini, V. Latora, M. Lucas, A. Patania, J.-G. Young, and G. Petri, Networks beyond pairwise interactions: Structure and dynamics, Phys. Rep. **874**, 1 (2020).

[15] T. Tanaka and T. Aoyagi, Multistable Attractors in a Network of Phase Oscillators with Three-Body Interactions, Phys. Rev. Lett. **106**, 224101 (2011).

[16] M. Komarov and A. Pikovsky, Finite-size-induced transitions to synchrony in oscillator ensembles with nonlinear global coupling, Phys. Rev. E **92**, 020901(R) (2015).

[17] C. Xu and P. S. Skardal, Spectrum of extensive multiclusters in the Kuramoto model with higher-order interactions, Phys. Rev. Res. **3**, 013013 (2021).

[18] X. Wang, Z. Zheng, and C. Xu, Collective dynamics of phase oscillator populations with three-body interactions, Phys. Rev. E **104**, 054208 (2021).

[19] P. S. Skardal and A. Arenas, Abrupt Desynchronization and Extensive Multistability in Globally Coupled Oscillator Simplexes, Phys. Rev. Lett. **122**, 248301 (2019).

[20] P. S. Skardal and A. Arenas, Higher order interactions in complex networks of phase oscillators promote abrupt synchronization switching, Commun. Phys. **3**, 218 (2020).

[21] M. Lucas, G. Cencetti, and F. Battiston, Multiorder Laplacian for synchronization in higher-order networks, Phys. Rev. Res. **2**, 033410 (2020).

[22] E. Ott and T. M. Antonsen, Low dimensional behavior of large systems of globally coupled oscillators, Chaos **18**, 037113 (2008).

[23] H. Chiba, Continuous limit and the moments system for the globally coupled phase oscillators, Discrete Contin. Dyn. Syst Ser. A **33**, 1891 (2013).

[24] N. Nakagawa and Y. Kuramoto, Collective chaos in a population of globally coupled oscillators, Prog. Theor. Phys. **89**, 313 (1993); P. Clusella and A. Politi, Between phase and amplitude oscillators, Phys. Rev. E **99**, 062201 (2019).

[25] V. Hakim and W. J. Rappel, Dynamics of the globally coupled complex Ginzburg-Landau equation, Phys. Rev. A **46**, R7347(R) (1992).

[26] P. C. Matthews and S. H. Strogatz, Phase Diagram for the Collective Behavior of Limit-Cycle Oscillators, Phys. Rev. Lett. **65**, 1701 (1990); P. C. Matthews, R. E. Mirollo, and S. H. Strogatz, Dynamics of a large system of coupled nonlinear oscillators, Phys. D (Amsterdam) **52**, 293 (1991).

[27] H. Bi, X. Hu, S. Boccaletti, X. Wang, Y. Zou, Z. Liu, and S. Guan, Coexistence of Quantized, Time Dependent, Clusters in Globally Coupled Oscillators, Phys. Rev. Lett. **117**, 204101 (2016); J. Zhang, S. Boccaletti, Z. Liu, and S. Guan, Synchronization of phase oscillators under asymmetric and bimodal distributions of natural frequencies, Chaos, Solitons Fractals **136**, 109777 (2020).

[28] See Supplemental Material at http://link.aps.org/supplemental/10.1103/PhysRevE.105.L042201 for the numerical evidence of collective chaos, the derivation of Eq. (2), and the calculation of the stability boundary of the UIS in Eqs. (1) and (2).

[29] M. C. Cross, J. L. Rogers, R. Lifshitz, and A. Zumdieck, Synchronization by reactive coupling and nonlinear frequency pulling, Phys. Rev. E **73**, 036205 (2006).

[30] A complete derivation can be found in the Supplemental Material. In Eq. (2), terms of orders $O(\epsilon^3)$ and $O(\epsilon^2\sigma)$ have been neglected, since small coupling strength ($\epsilon \ll 1$) and frequency dispersion ($\sigma \ll 1$) are assumed. Moreover, note that phase reduction does not introduce terms proportional to $\epsilon\sigma$, as in Ref. [33].

[31] H. Daido, Critical conditions of macroscopic mutual entrainment in uniformly coupled limit-cycle oscillators, Prog. Theor. Phys. **89**, 929 (1993).

[32] Y. Kuramoto and H. Nakao, On the concept of dynamical reduction: the case of coupled oscillators, Philos. Trans. R. Soc. A **377**, 20190041 (2019).

[33] E. Gengel, E. Teichmann, M. Rosenblum, and A. Pikovsky, High-order phase reduction for coupled oscillators, J. Phys.: Complexity **2**, 015005 (2021).

[34] Notice these identities: $R^2 \sin(2\Psi - 2\theta_j + \beta) = N^{-2}\sum_{k,l}\sin(\theta_k + \theta_l - 2\theta_j + \beta)$; $RQ\sin(\Phi - \Psi - \theta_j) = N^{-2}\sum_{k,l}\sin(2\theta_k - \theta_l - \theta_j)$.

[35] H.-W. Hammer, A. Nogga, and A. Schwenk, Colloquium: Three-body forces: From cold atoms to nuclei, Rev. Mod. Phys. **85**, 197 (2013).

[36] C. Bick, P. Ashwin, and A. Rodrigues, Chaos in generically coupled phase oscillator networks with nonpairwise interactions, Chaos **26**, 094814 (2016).

[37] P. S. Skardal and A. Arenas, Memory selection and information switching in oscillator networks with higher-order interactions, J. Phys.: Complexity **2**, 015003 (2021).

[38] M. Kumar and M. Rosenblum, Two mechanisms of remote synchronization in a chain of Stuart-Landau oscillators, Phys. Rev. E **104**, 054202 (2021).

[39] O. V. Popovych, Y. L. Maistrenko, and P. A. Tass, Phase chaos in coupled oscillators, Phys. Rev. E **71**, 065201(R) (2005).

[40] M. Abramowitz and I. A. Stegun, *Handbook of Mathematical Functions* (Dover, New York, 1972).

[41] D. Rand, Dynamics and symmetry. Predictions for modulated waves in rotating fluids, Arch. Ration. Mech. Anal. **79**, 1 (1982).

[42] D. Barkley, Euclidean Symmetry and the Dynamics of Rotating Spiral Waves, Phys. Rev. Lett. **72**, 164 (1994).

[43] I. León and D. Pazó, Quasi phase reduction of all-to-all strongly coupled $\lambda - \omega$ oscillators near incoherent states, Phys. Rev. E **102**, 042203 (2020).